Photonik
Ingenieurbüro
Dr. Walter Luhs

Manual
PE-0400 Diffraction of Light

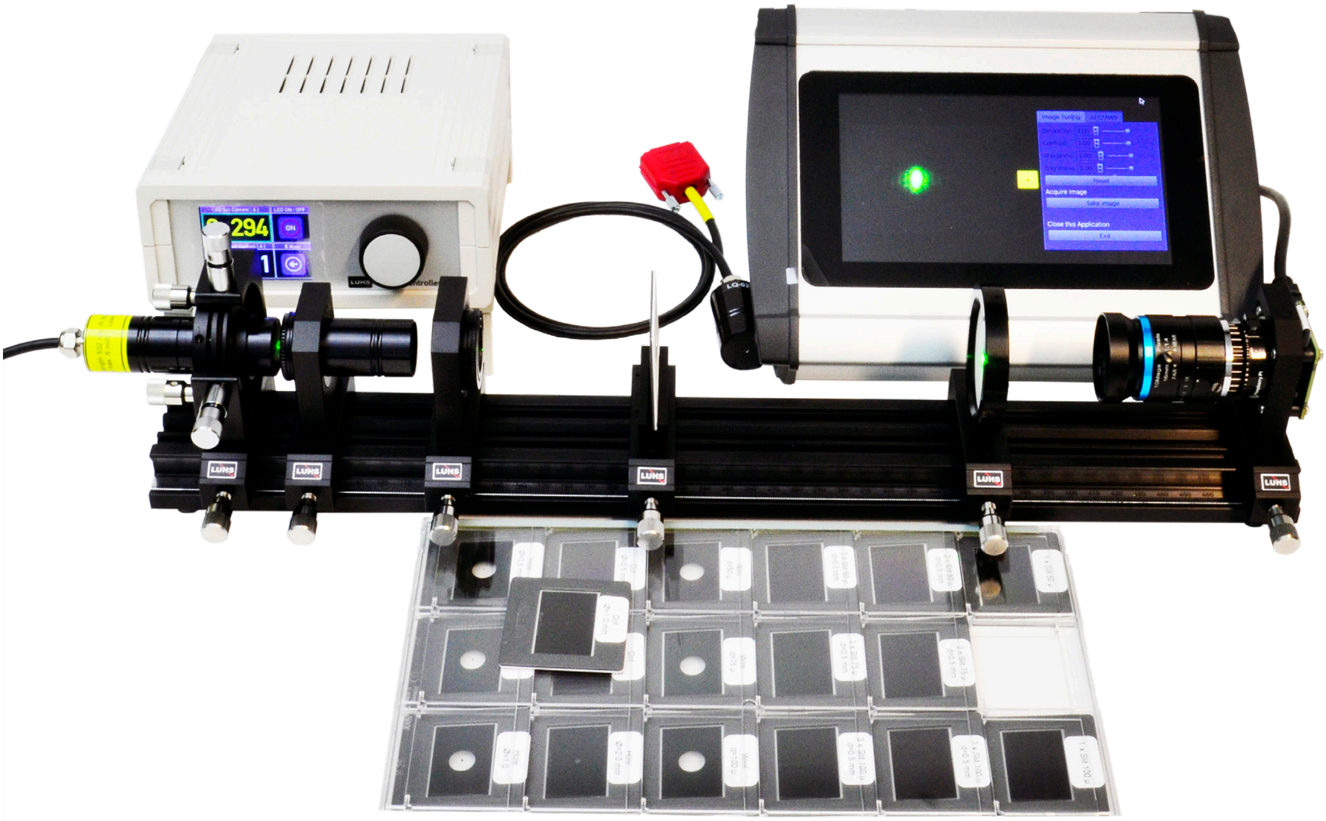

Table of Contents
Introduction
Theory
Experimental Setup
Measurements

Table of Contents

1.0 Introduction

All objects which restrict the free propagation of light cause diffraction. Although this phenomenon is always present, it is usually neglected, because the effect is too insignificant for the topic of investigation. However, if light hits sharp edges, diffraction will appear clearly and cannot be neglected, especially when light is diffracted on very narrow openings like holes or slits. Christian Huygens formulated his observation of diffraction in the 17th century, applying the principle of elementary waves. In 1800, Fresnel and Fraunhofer both studied the effect of diffraction in detail. Fresnel used divergent light for his investigations, whereas Fraunhofer used parallel light created by a pair of lenses. Both techniques are termed as Fresnel and Fraunhofer diffraction, respectively. This experiment offers both types of diffraction. Experiments are performed using monochromatic laser light, which will be diffracted at slits and holes of various widths. Thin wires impressively prove the Babinet theorem which states that complementary masks (slit, wire) result in the same diffraction pattern. The obtained diffraction patterns are imaged on a white screen, and a CCD camera can also record the pattern.

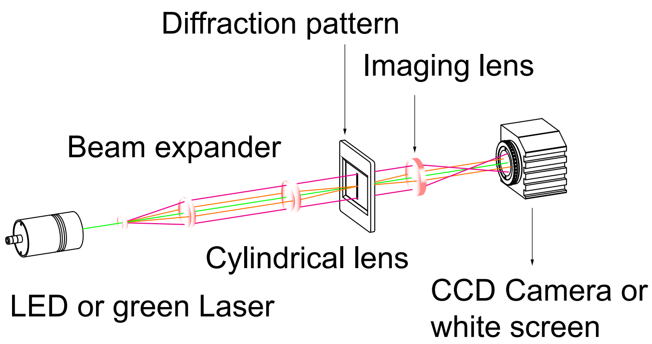

Fig. 1: Principle set-up

The experiment uses a red-emitting LED or a green-emitting laser. For both light sources, the controller provides the individual current and voltage. The controller's microprocessor reads the property of the connected light source and sets the parameter accordingly. When using the green laser and a vertical slit or wire, the beam expander is needed to create a vertical line shape in conjunction with the cylindrical lens. Different types of diffraction elements can be inserted into the plate holder. To verify Babinet's theorem, a slit and a wire with the same dimensions are used. Furthermore, the diffraction fringes, a double slit, a circular aperture, and a two-dimensional structure are created and recorded. For a first view, the translucent screen is used. The fringes on the screen are recorded by the high-resolution (13 MP) CCD camera and are displayed live on the digital video controller. The image can be taken as a still photo, as a video, or a data file. The video controller provides USB inputs for a memory stick or other external devices like a mouse or keyboard.e and a two dimensional structure are created and recorded. For a first view, the translucent screen is used. The fringes on the screen are recorded by the high resolution (13 MP) CCD camera and are displayed live on the digital video controller. The image can be taken as still photo, as video or data file. The video controller provides USB inputs for a memory stick or other external devices like mouse or keyboard.

2.0 Multiple beam interference

After joining the Royal Society of London in 1672, Newton stated light is made of particles and not waves.
Newton's corpuscular theory of light is based on the following points

1. Light consists of very tiny particles known as "corpuscular".
2. These corpuscles on emission from the source of light travel in straight line with high velocity
3. When these particles enter the eyes, they produce image of the object or sensation of vision.
4. Corpuscles of different colours have different sizes.

In 1679, Christian Huygens proposed the wave theory of light.
According to Huygen's wave theory:

1. Each point of a light source sends out waves in all directions in a hypothetical medium called "ETHER".
2. Light is a form of energy
3. Light travels as waves.
4. Like for sound in air a medium is necessary for the propagation of waves and the whole space is filled with such an "Ether"
5. Compared to sound, light waves have very short wave length

Already at this time the battle about the property of light was initiated. Newton enjoyed the absolute scientific authority and one can imagine what Huygens dared to claim.

"There remained one problem that Huygens theory of light could not solve. In 1669, three years before Newton first presented his particle theory of light, Danish physicist Erasmus Bartholin had begun experimenting with transparent calcite crystals that had been discovered in Iceland. He found that when an image is placed behind a crystal it is duplicated, with one copy appearing slightly higher than the other."

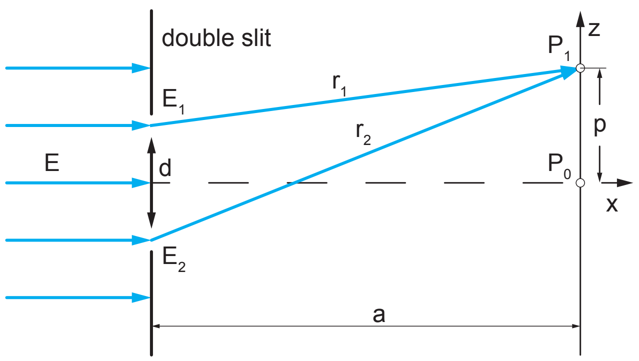

Fig. 2: Thomas Young's double slit experiment of 1802

The basic idea of the analysis of the interference is to calculate for the path difference Δ of the interfering rays. In the example of the Fig. 2 we note:

$$\Delta = r_2 - r_1$$

$$r_1^2 = a^2 + \left(p - \frac{d}{2}\right)^2$$

$$r_2^2 = a^2 + \left(p + \frac{d}{2}\right)^2$$

$$r_2^2 - r_1^2 = 2 \cdot p \cdot d = (r_2 - r_1) \cdot (r_2 + r_1)$$

$$p, d \ll a$$

$$r_1 + r_2 \approx 2 \cdot a$$

$$2 \cdot p \cdot d = (r_2 - r_1) \cdot 2 \cdot a$$

$$\Delta = r_2 - r_1 = \frac{p \cdot d}{a}$$

$$\delta = \frac{2 \cdot \pi}{\lambda} \cdot \Delta = \frac{2 \cdot \pi}{\lambda} \cdot \frac{p \cdot d}{a}$$

From the previous chapter we learned that constructive superposition occurs, when

$$\delta = 0, \pm 2\pi, \pm 4\pi, ...$$

and destructive interference for:

$$\delta = \pm \pi$$

$$I(z) = \begin{cases} \max & 0, \quad \pm \frac{\lambda \cdot a}{d}, \quad \pm 2 \cdot \frac{\lambda \cdot a}{d}, ... \\ \min & \pm \frac{1}{2} \cdot \frac{\lambda \cdot a}{d}, \quad \pm \frac{3}{2} \cdot \frac{\lambda \cdot a}{d}, \quad \pm \frac{5}{2} \cdot \frac{\lambda \cdot a}{d}, ... \end{cases}$$

Thomas Young performed his famous Double Slit Experiment in 1802. From his results and conclusions, it was determined that light propagates in wave form and therefore possesses the ability to interfere with itself. Young also is responsible for the principle of coherence and of superposition, two of the most fundamental principles in the fields of interferometry and optics. Thus, the wave theory of light came to be thanks to the refinement efforts of several distinguished and important people.
During the gold-rush mood of the wave nature of light a variety of observations and interference schemes came up.
Arago, Fizeau and Foucault interference of light at thin wedges (1848), almost during same time Haidinger fringes, interference of equal inclination.
In principle a lot of possible interference schemes can be conceived. To analyze such a scheme simply the superimposition of waves it is useful to identify the interfering electrical field vector $\vec{E}$.

$$\vec{E}_i = \vec{E}_a + \vec{E}_b$$

$$I(x,y,z) = \left|\vec{E}_i\right|^2 = \left|\vec{E}_a + \vec{E}_b\right|^2$$

Theory

3.0 Diffraction

In all cases where an object has nearly the same dimension of the wavelength of the light with which the object interacts, the diffraction phenomena are dominating instead of geometrical considerations.

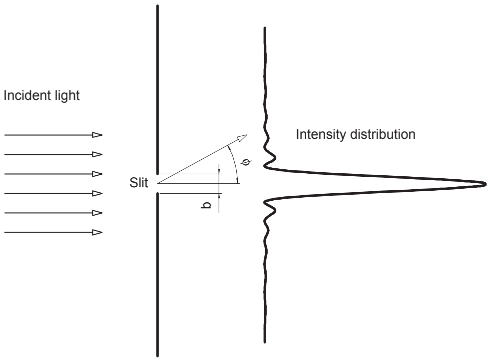

Fig. 3: Diffraction at a slit with a width of b

This becomes clear if one looks at the bottom surface of a CD, one notices the occurrence of rainbow colors. Beside that the CD also acts as a mirror. Thus we can conclude, that a CD acts as a reflecting grating. If no pits where printed to the CD it would act only as a simple mirror. To understand why the back reflected intensity of the incident laser beam is changed when it hits a bump (pit) we have to recall the diffraction at a slit.

Actually the CD has no slits, but the description of a slit with a mirror behind it is equivalent. In a first step we neglect the height of the bump. From basic physics textbooks we learn that the intensity distribution of the light behind a slit can be written as:

$$I(\phi) \sim b^2 \cdot \frac{\sin^2\left(\frac{\pi \cdot b}{\lambda} \cdot \sin\phi\right)}{\left(\frac{\pi \cdot b}{\lambda} \cdot \sin\phi\right)^2}$$

(Eq 1.1)

If the width of the slit b is large compared to the wavelength λ of the incident beam we will obtain an intensity distribution as shown in Fig. 4 A. When we are going to decrease the width of the slit towards b=λ we will get an intensity distribution like Fig. 4 B. For the case of the CD we can conclude that due to the now broad intensity distribution only a small part of the back reflected light will enter the aperture of the pick-up optics resulting in a reduction of the reflected intensity. The light which shines beside the bump is simply reflected back and enters without change of direction and intensity the pick-up optics. Both the reflected light from the bump as well the light around it are in phase. If we introduce a phase shift of 90° (λ/2) between both light beams destructive interference occurs resulting in a further decrease of the back reflected light intensity. For this reason the height of the reflecting bump is chosen to be λ/4.

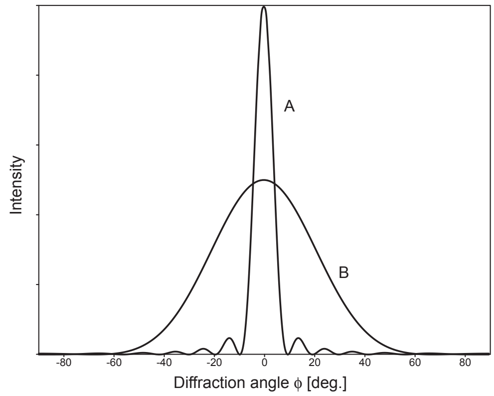

Fig. 4: Intensity distribution for a width of the slit A) b = 6 λ and B) b = λ

In summary the change of back reflected intensity when the laser beam hits a bump is due to diffraction and interference. In the next fig. 2.40 the situation is shown to illuminate the phenomena of interference.

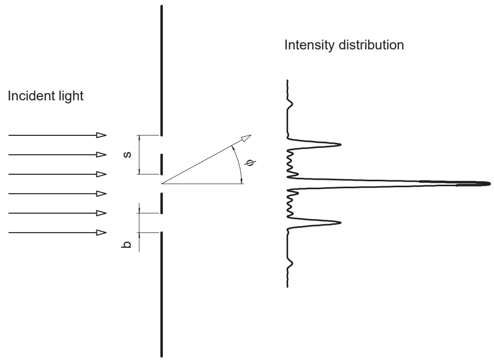

Fig. 5: Diffraction with two slits having a width of b and a distance of s

If we are going to increase the number p of slits the intensity distribution behind the slit can be expressed as:

$$I(\phi) \sim \frac{\sin^2\left(\frac{\pi \cdot b}{\lambda} \cdot \sin\phi\right)}{\left(\frac{\pi \cdot b}{\lambda} \cdot \sin\phi\right)^2} \cdot \frac{\sin^2\left(\frac{\pi \cdot p}{\lambda} \cdot s \cdot \sin\phi\right)}{\sin^2\left(\frac{\pi}{\lambda} \cdot s \cdot \sin\phi\right)}$$

In fig. 2.43 this function is represented. For a given wavelength λ the grating can be optimized in such a way that the intensity distribution now consists of three distinct maxima.

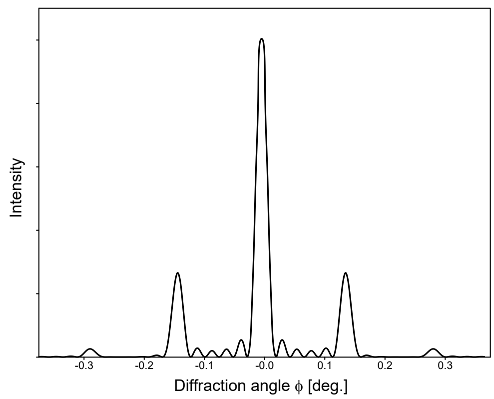

Fig. 6: Three beam intensity distribution generated by a for this purpose designed grating

4.0 Description of Components and Setup

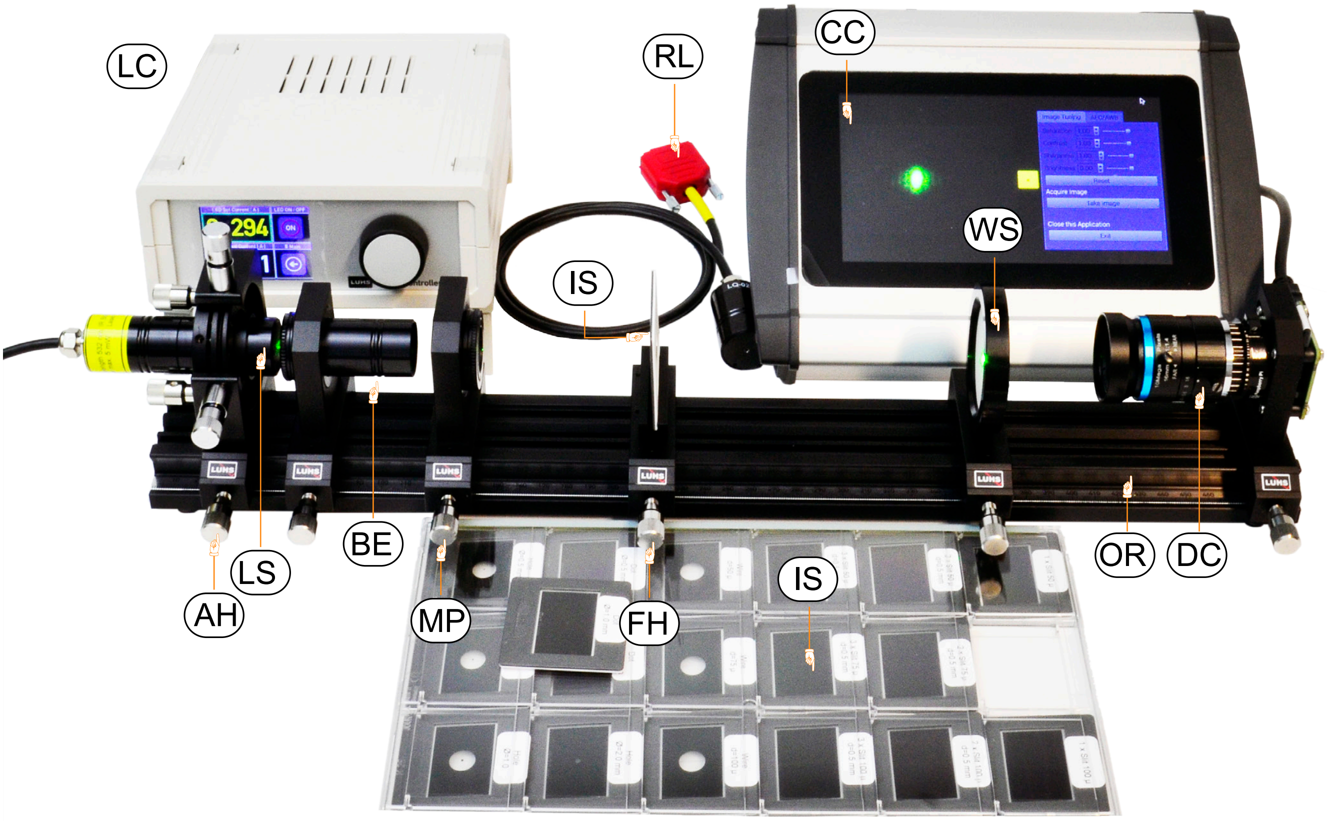

4.1 (LC) LED and Laser Controller

This microprocessor operated device contains an LED current controller and optional a photodiode amplifier. A touch panel display allows in conjunction with the digital knob the selection and setting of the parameters for the attached LED or photodiode. The controller reads the operation values of the connected LED or laser from the EEPROM located inside its connector. The device comes with a 230 VAC / 12 VDC wall plug power supply.

The controller is operated by 12 VDC via the provided wall plug power supply. The LED or laser are connected via the 15 pin SubD connector labelled "LED/LD". When the LED or laser is operated in modulated mode, the reference modulator signal is available at the "MODULATOR" BNC connector.

When the external 12 V is applied and switched on, the controller starts displaying the screen as shown in the figure above.

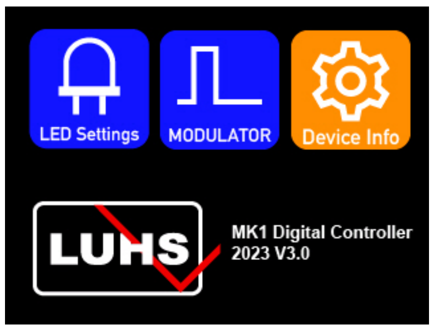

After touching the start screen the upcoming interactive screen appears with the selection of 3 buttons:

F. LED/Laser current settings
G. Modulation of the LED/laser
H. Device and LED/laser information

Touching the LED Settings button brings up the current settings page.

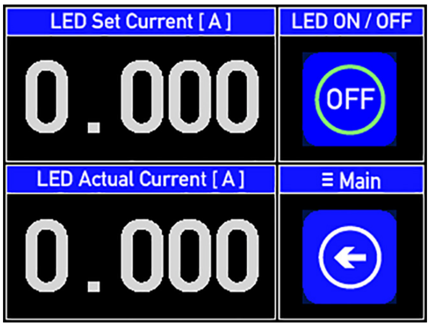

The current settings screen shows the set current as well as the actual current. With the LD ON/OFF touch button the laser is switched on or off. The ≡Main touch button switches back to the main page.

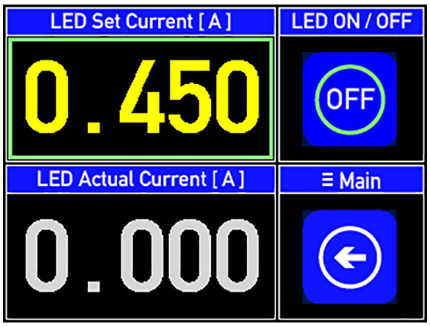

By touching the “LED Set Current” display field it is highlighted. By turning now the settings knob, the value of the injection current can be set and is immediately applied, provided the LED ON/OFF touch button is activated.

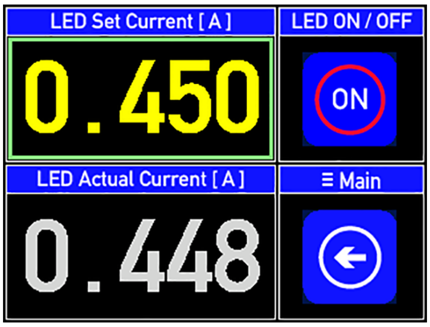

Touching the LED ON/OFF button switches the LED ON or OFF. When switched ON, the actual current is displayed in addition.

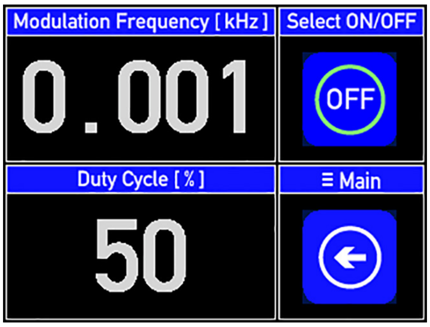

The LED or laser can be switched periodically on and off. This is for a couple of experiments of interest.

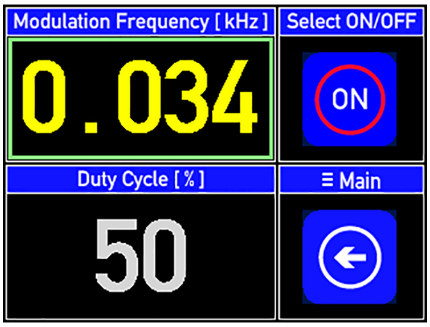

By tapping the display of the modulation frequency the entry is activated. Turning the settings knob will set the desired frequency value. The modulation becomes active, when the Modulator ON/OFF button is tapped.

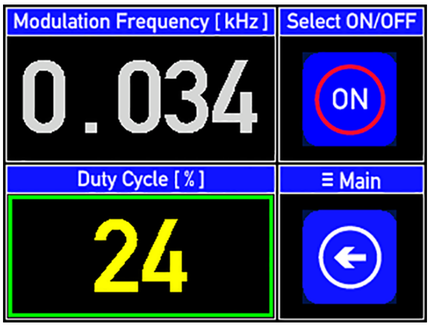

For some experiments it is important to keep the thermal load on the optically pumped object as low as possible or to simulate a flash lamp like pumping. For this reason the duty cycle of the injection current modulation can be changed in a range of 1...100 %. A duty cycle of 50% means that the OFF and ON period has the same length. The set duty cycle is applied instantly to the injection current controller.

This screen appears only, when no LED or laser is connect to the device

4.2 (AH) Four axes adjustment holder

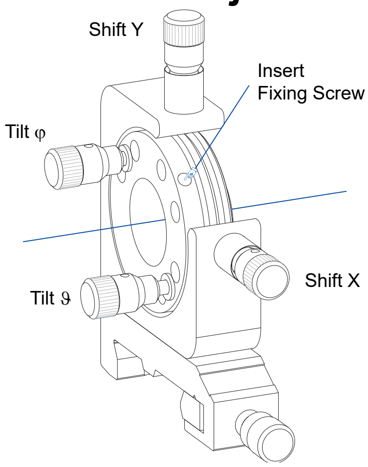

This frequently needed component is ideal for the fine adjustment of lenses, microscope objectives, diode laser, and so on for the optical axis of the rail set-up. The displacement area is 5x5 mm and 10x10 degrees, respectively. Different mounts can be attached to the adjustment holder. This model provides a holder for 25 mm cylindrical components. The component is inserted into the adjustment holder and is kept in position by a grub screw with a nylon tip. Four precise fine-pitch screws of repetitious accuracy allow the translational (X; Y) and azimuthal (υ; φ) adjustment.

4.3 (LS) The Light Source

4.3.1 Red Light LED

White LED in ø 25 Housing

A red light LED is built into a round housing (C25). The LED is connected via a 15 pin SubD HD connector to the controller MK1. Inside the connector an EPROM contains the data of the LED and when connected to the controller, these data are read and displayed by the controller.

4.3.2 Green Laser

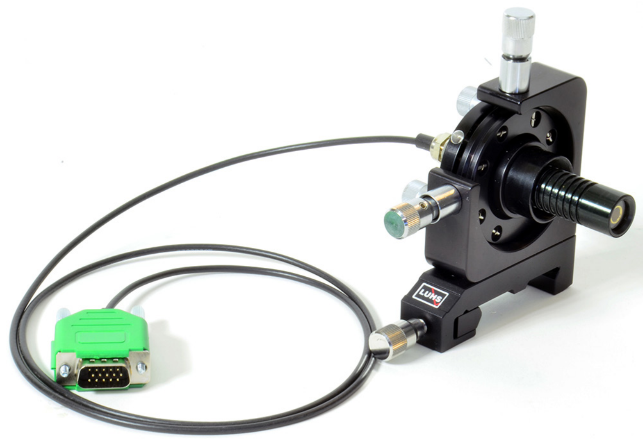

Green (532 nm) DPSSL in ø25 housing inserted into the 4 axes adjustment holder (depending on available models the appearance may vary slightly)

A green (532 nm) emitting DPSSL (Diode Pumped Solid State Laser) is integrated into a C25 housing and is operated with the "DC-0020 LED Controller". The output power is less 5 mW. An integrated filter blocks the 808 nm and 1064 nm). The laser is connected via a 15 pin SubD HD connector to the controller. Inside the connector an EEPROM contains the data of the laser diode and when connected to the controller, these data are read and displayed by the controller.

4.4 (MP) Mounting Plate

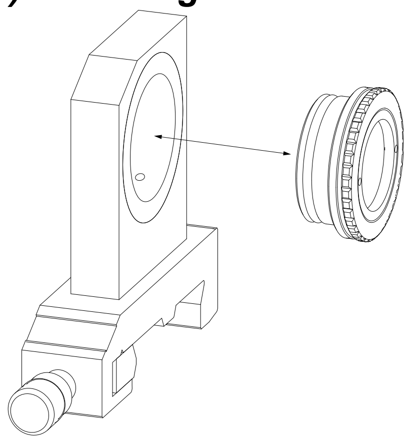

This frequently used component is ideal to accommodate parts with a diameter of 30 or 25 mm where it is kept in position by three spring loaded steel balls. Especially C25 or C30 mounts having a click groove are firmly pulled into the mounting plate due to the smart chosen geometry. The mounting plate is mounted to a 20 mm wide carrier.

4.5 (BE) Beam Expander

Beam Expander x6 in ø25 housing

The beam expander is based on a Galilean telescope with one concave lens as entry lens and a plano-convex as exit lens. The expansion ratio is defined by the ratio of the focal length of the lenses. The entry lens is mounted into a C25 mount which screwed to the 25 mm housing at which end the exit lens is mounted. This beam expander has an expansion rate of 6. The telescope is aligned for far sight view and can be slightly changed by turning the C25 mount to change the parallel wave front into curved ones.

The beam expander is used to enlarge the laser beam to provide an almost parallel beam of coherent light.

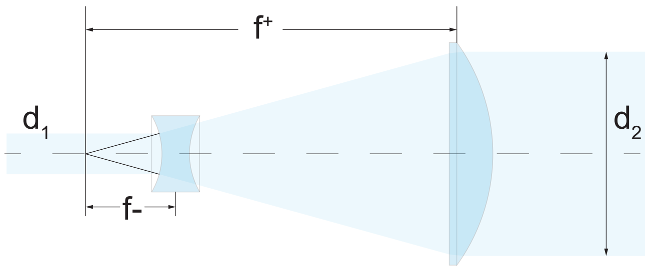

Fig. 7: Galilean beam expander

Expansion ratio or magnification:

$$\frac{d_2}{d_1} = \frac{f^+}{f^-}$$

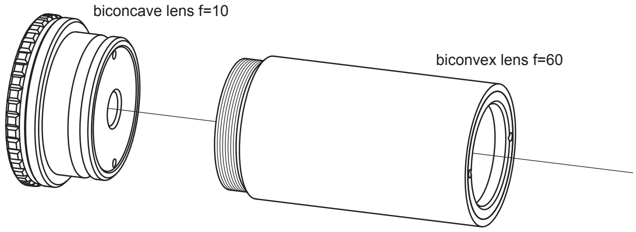

The provided beam expander consists of a combination of a biconcave (f=-10) and biconvex lens (f=60) forming the so called Galilean beam expander with a magnification of 6. The beam expander can be separated in such a way that the lenses can be used independently.

4.6 (KH) Filter plate holder

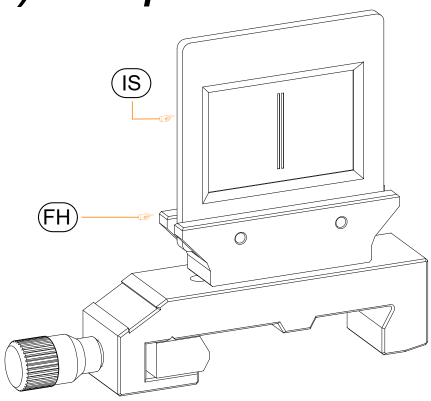

This filter plate holder is designed to accommodate standard optical filter plates with a thickness of 3 mm, a width of 50 mm and a height of 50 mm. The inserted plate is held in position by two grub screws which have spring loaded balls at their tips.

4.7 (WS) Translucent White Screen

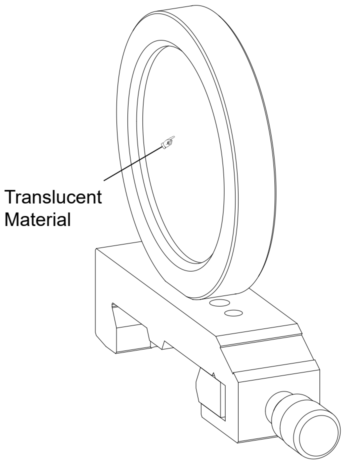

Translucent screen on carrier MG20

In a round holder a sheet of translucent paper is fixed with a retaining ring. This component is useful to image and visualize optical rays. Furthermore, the translucence allows the convenient photographic recording from the opposite side with digital cameras for a quick picture for the students measurement report.

4.8 (OR) Optical Rail

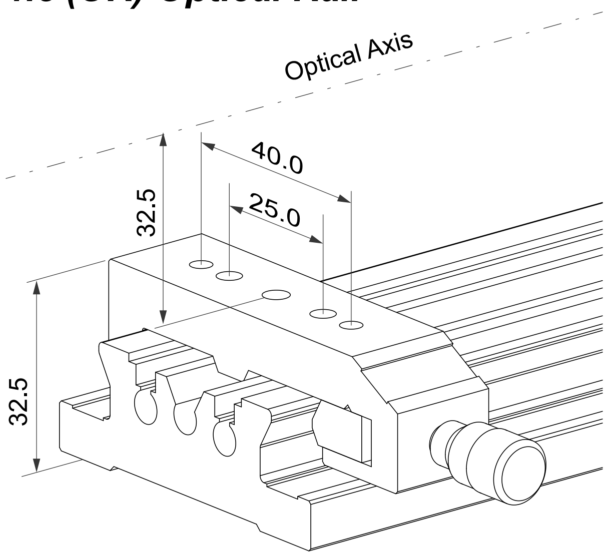

Rail and carrier system

The rail and carrier system provides a high degree of integral structural stiffness and accuracy. Due to this structure it is a further development optimised for daily laboratory use.

The optical height of the optical axis is chosen to be 65 mm above the table surface. The optical height is 32.5 mm above the carrier surface.

4.9 (CC) Camera Controller

The camera controller uses a Raspberry Pi 4 computer with the standard Linux distribution. The display is the recommended Raspberry 7-inch display.

The communication ports of the Raspberry PI are located at the rear of the housing, like USB 2.0 and USB 3.0, as well as network access. The camera will be connected via a mini HDMI connector.

For the operation of the camera controller, the USB-C connector is provided to connect to an external wall plug power supply. Connect the provided mouse and keyboard to the USB 2.0 ports. The Raspberry PI boots to the desktop screen once the camera and the USB-C power supply are connected. In the start menu, you will select the “LUHS” application. The code is written in Python and is located in the folder home/LUHS/Camera.

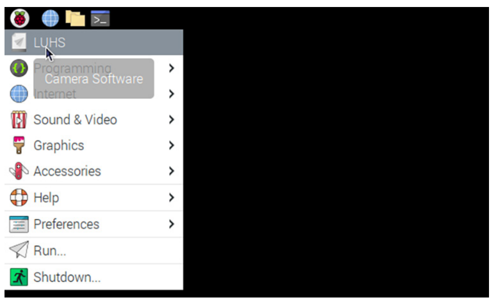

Select and run the application “LUHS” in the start menu

The screen shows the camera pictures and a yellow button. A click on it will shift the settings tabs into the scene.

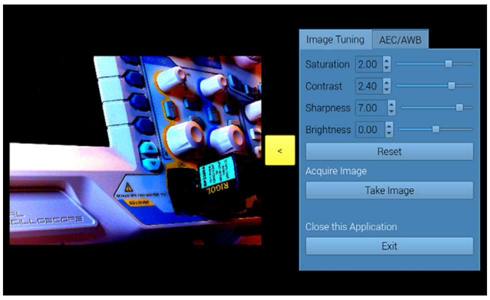

The settings tabs are divided into two sections. One is used to manipulate the image properties like saturation, brightness, contrast, and sharpness.

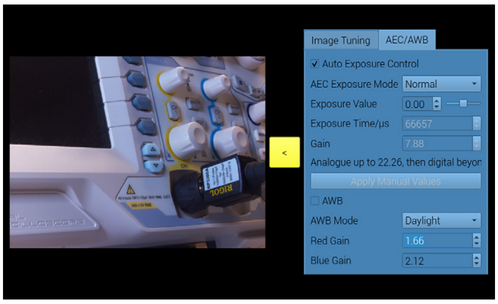

The other relates to AEC (Automatic Exposure Control) and AWB (Automatic White Balance), providing a wide variety to find the best setting for the image.

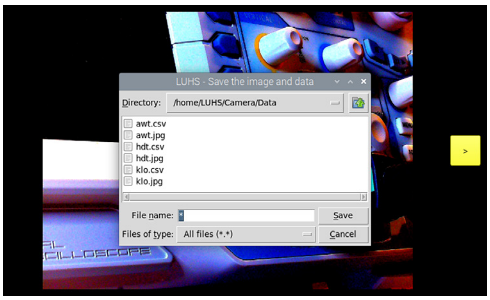

After finding the optimum image settings, the image can be saved to the camera controller's memory or an attached USB stick. Besides the jpeg image file, a CSV data file is created and stored. The CSV data file contains the intensity for each pixel (4056 x 3040) of the CCD chip of the camera. The CSV file allows the latter numerical evaluation of the image.

4.10 (DC) Digital Camera

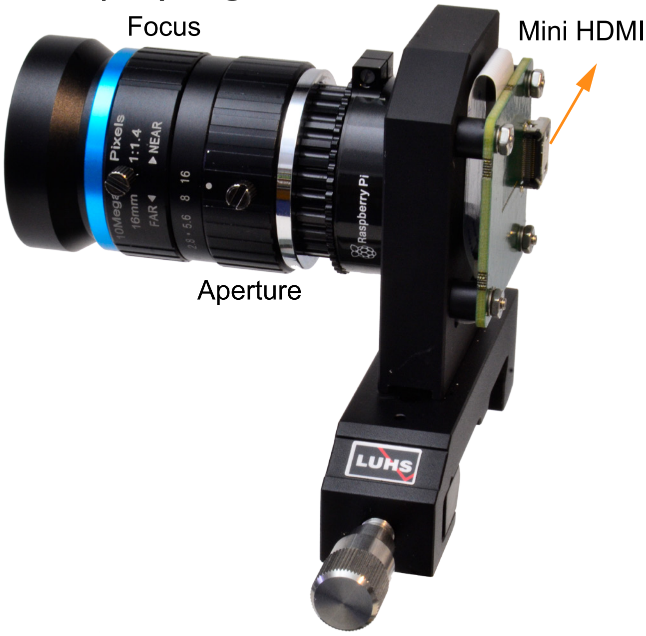

The official Raspberry 12 MB camera is integrated into a housing attached to a carrier. The center of the chip is in line with the optical axis of the setup. The camera chip is connected via a mini HDMI cable to the controller. The objective is optimized for the CCD chip and has focus and aperture adjusting rings. The camera uses the Sony IMX477R chip with a pixel size of 1.55 µm × 1.55 µm. The entire sensor has a 7,564 × 5.476 mm dimension, having 4056 ×3040 separate pixels.

5.0 Setup and Measurement

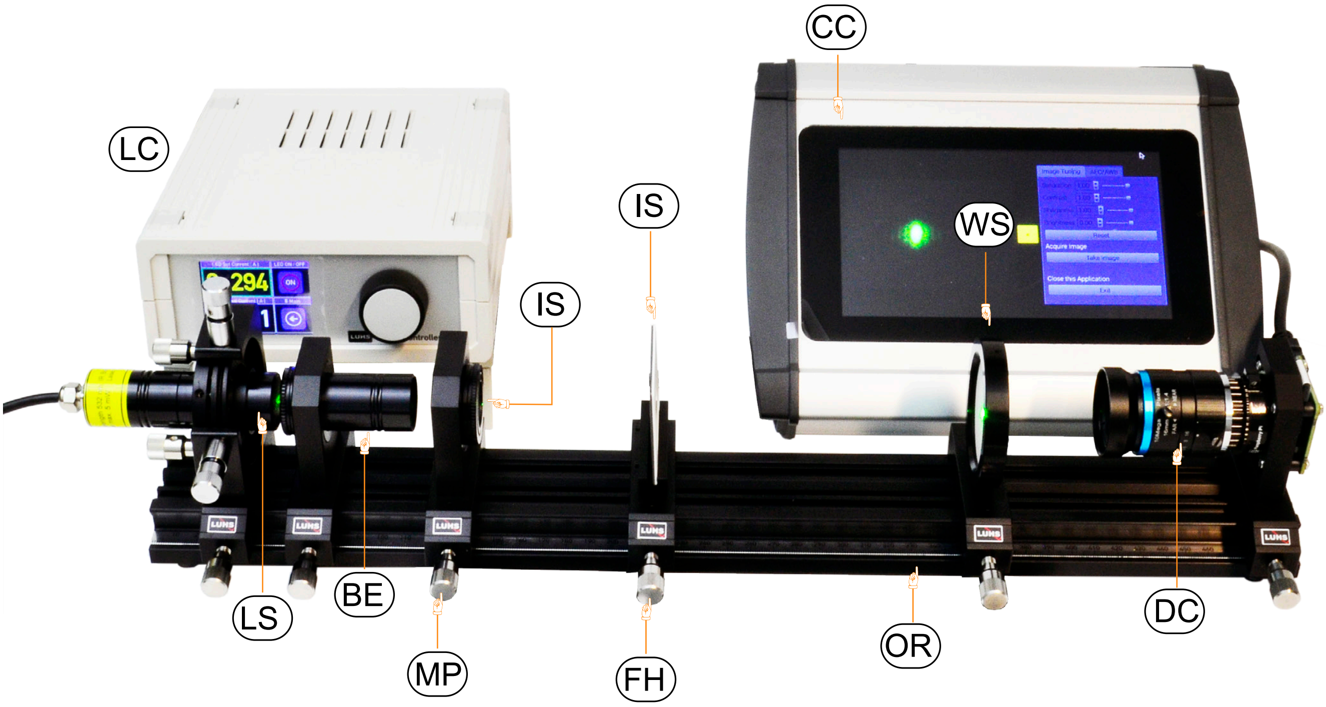

In front of the laser light source, which is the green laser in this setup, we place the beam expander (BE). We use only the white screen (WS) in the first setup. The digital camera is located behind the white screen. The focus and aperture are set for a crisp image. The image of the free-propagating green laser beam is shown in Fig. 8. It shows the typical Gaussian beam distribution. Next, we add a slit, starting with a slit width of 50 µm. The Fig. 9 shows the image with appearing interference or diffraction fringes. The following Fig. 10 and Fig. 11 have been taken with wider slits, 75 µm, and 100 µm.
Others can be used and analyzed from the set of diffraction patterns (SI).

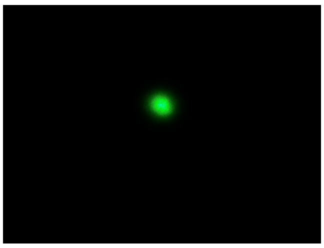

Fig. 8: Without slit

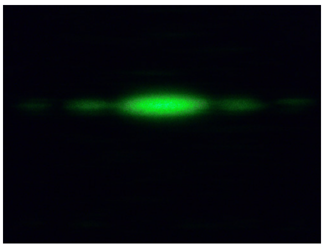

Fig. 9: 50 µm slit

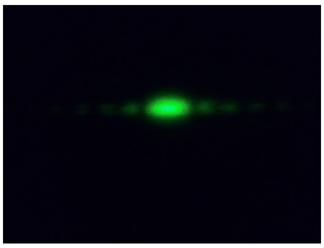

Fig. 10: 75 µm slit

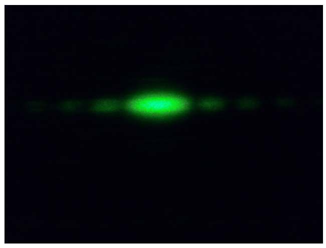

Fig. 11: 100 µm slit

So far, we have yet to discuss the prerequisites for the appearance of diffraction or interference. We assumed the incident light has just one sharp wavelength L in all related equations. However, only a coherent light source like the laser comes close to this assumption. Looking at (Eq 1.1), we notice that the intensity maxima shifts for another wavelength, and if we consider a large number of wavelengths, the structure smears out. No diffraction structure is visible any longer. We use a red LED instead of a green laser to verify this phenomenon. To obtain a vertical line to illuminate the slit, we use the cylindrical lens with a focal length of 80 mm. The beam expander (BE) is not used in this setup.

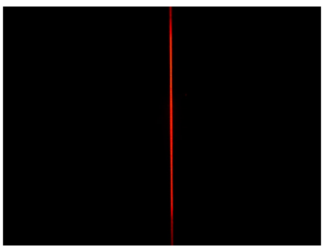

Fig. 12: 1 x 50 µm slit

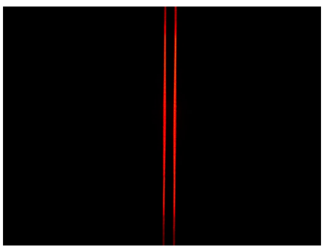

Fig. 13: 2 x 50 µm slit d=0.5 mm

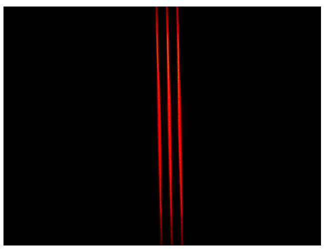

Fig. 14: 3 x 50 µm slit d=0.5 mm

The fig 12-14 show the image of the slits when illuminated with a red LED. No diffraction patterns are visible; only the slit as such is imaged. The width of the slit is 0.050 mm, and if there is more than one, the distance to each other is 0.5 mm. We get a precise calibration procedure for the camera image using this information and the given dimensions of the CCD chip.

5.1 Image analysis

As mentioned, saving an image, a JPEG graphics file is saved, and the intensity matrix is written into a CSV file. The Fig. 15 shows the content of the JPEG image, whereas the Fig. 16 shows the intensity distribution calculated from the CSV file.

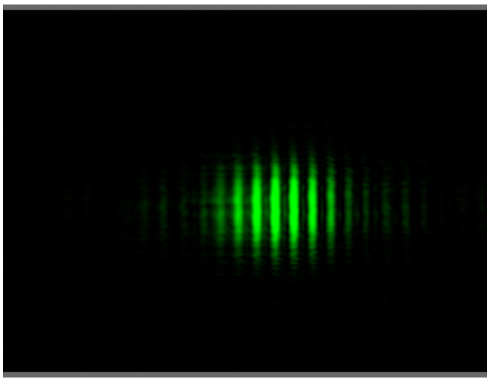

Fig. 15: Image of the save JPEG file

There are a variety of software available to evaluate numerical data. Everybody has their favorites. MatLab, for instance, is often used. In our case, we made a short program written in Visual Basic.

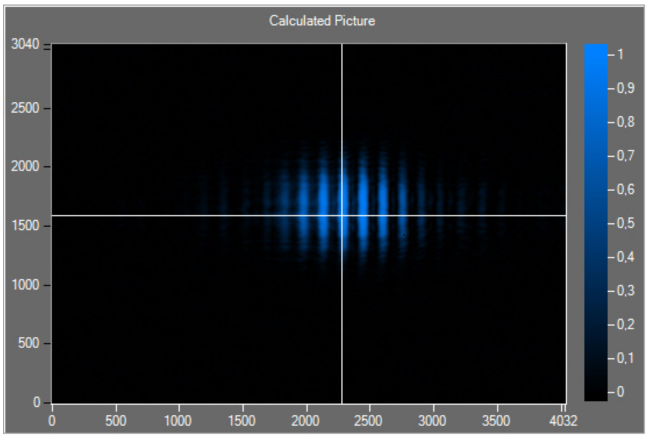

Fig. 16: Content of the CSV matrix file

The CSV file does not contain any color information. Each matrix element gives the intensity in values from 0 to 255 of the selected pixel. Any other color to display the intensity distribution can be selected.

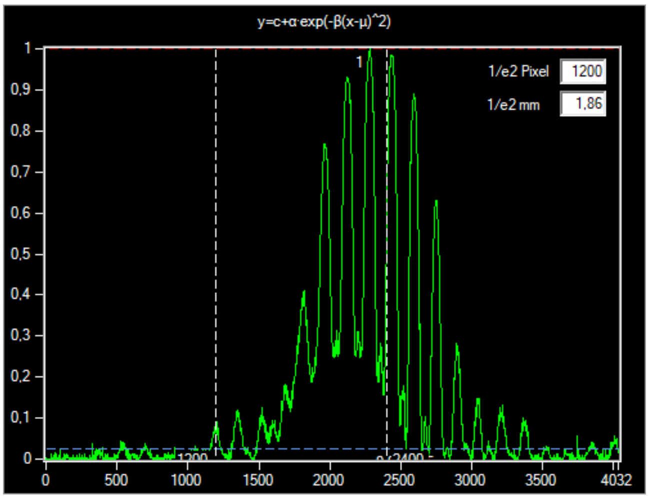

Fig. 17: Intensity distribution along the horizontal axis of Fig. 16